Improved Water and Lipid Suppression for 3D PRESS CSI Using RF Band Selective Inversion with Gradient Dephasing (BASING)

Josh Star-Lack, Sarah J. Nelson, John Kurhanewicz, L. Royal Huang, Daniel B. Vigneron

A T_1 insensitive solvent suppression technique—band selective inversion with gradient dephasing (BASING)—was developed to suppress water and lipids for ^{1}H magnetic resonance spectroscopy (MRS). BASING, which consists of a frequency selective RF inversion pulse surrounded by spoiler gradient pulses of opposite signs, was used to dephase stopband resonances and minimally impact passband metabolites. Passband phase linearity was achieved with a dual BASING scheme. Using the Shinnar-Le Roux algorithm, a highpass filter was designed to suppress water and rephase the lactate methyl doublet independently of *TE*, and water/lipid bandstop filters were designed for the brain and prostate. Phantom and *in vivo* experimental 3D PRESS CSI data were acquired at 1.5 T to compare BASING with CHESS and STIR suppression. With BASING, the measured suppression factor was over 100 times higher than with CHESS or STIR causing baseline distortions to be removed. It was shown that BASING can be incorporated into a variety of sequences to offer improved suppression in the presence of B_1 and T_1 inhomogeneites.

Key words: magnetic resonance spectroscopy (MRS); water and lipid suppression; ^{1}H PRESS CSI; RF pulse design.

INTRODUCTION

In vivo ^{1}H chemical shift imaging (CSI) (1, 2) may suffer from inadequate water and/or lipid suppression resulting in baseline distortions and inaccurate estimates of spectral intensity. In CSI studies of brain and prostate tumors (3–5) using PRESS localization (6), we have found that the most commonly used suppression techniques—CHESS (7) and STIR (8)—can be too sensitive to local T_1 and/or B_1 variations to be adequate. Although optimized CHESS sequences (9, 10) can reduce these dependencies, we sought a more general approach that is less sensitive to the range of T_1 values and B_1 inhomogeneities inherent in different experimental setups.

MRM 38:311–321 (1997)

From the Magnetic Resonance Science Center, Department of Radiology, Box 1290, University of California, San Francisco, California.

Address correspondence to: Daniel B. Vigneron, Ph.D., Magnetic Resonance Science Center, Department of Radiology, Box 1290, University of California, San Francisco, CA 94143.

Received July 31, 1996; revised February 25, 1997; accepted February 26, 1997.

This work was supported by NIH grants CA57236, CA59880, CA59897, and American Cancer Society Grant #EDT-34.

Current address for J.S-L.: Lucas MRS Building, Department of Radiology, Stanford University, MC5488, Stanford, CA 94305.

Portions of this work were presented at the ISMRM Fourth Scientific Meeting in New York (Abstract #194).

0740-3194/97 $3.00

Copyright © 1997 by Williams & Wilkins
All rights of reproduction in any form reserved.

One means of obtaining T_1-insensitive water suppression is to incorporate a frequency selective 180° crushed spin-echo (SE) pulse to flip and rephase the on-resonance passbands, which include the metabolites of interest and exclude the moieties to be suppressed (11, 12). Previous applications have been to noninterleaved 2D CSI where slice selection is achieved with the excitation pulse and is not required for the SE pulse. Although excellent suppression was achieved, this approach may not be optimal for a sequence such as PRESS, which already contains two SE pulses for spatial selection. The addition of frequency-selective SE pulses could potentially exacerbate B_1 dependent signal amplitude and phase variations across the volume of interest (VOI) and would complicate the echo-time dependence on RF pulse placement.

A practical alternative to frequency selective *rephasing* is frequency selective *dephasing*. Here, the suppression sequence is designed so that the stop band(s) (e.g., water and/or lipids) are placed on-resonance, acted upon by the RF field and dephased through the use of B_0 crusher gradients. An advantage of this approach is that the off-resonance passband metabolites are minimally impacted by the soft RF pulse. Dephasing techniques, which previously have been developed for suppression at high fields, include the single-echo WATERGATE (13) and MULTIGATE (14) sequences and dual-echo excitation sculpting (15). These methods are primarily applicable toward nonlocalized spectroscopy as the embedded SE pulses may not be slice selective as is required for PRESS localization.

To achieve our aims of obtaining T_1-independent suppression, robustness to B_1 inhomogeneities as well as spatial SE excitation, we developed a frequency-selective dephasing scheme—band selective inversion with gradient dephasing (BASING)—for long *TE* scans at 1.5 T. Using the Shinnar Le-Roux (SLR) algorithm (16–18) filters with sharp transition bands were designed to suppress water and lipids. Our results also show that BASING may have unique applications for visualizing weakly coupled spins.

This paper first derives the theoretical excitation profile of the BASING pulse and describes the design methodology. Several design examples are then provided along with CSI phantom and *in vivo* results obtained with BASING incorporated into the PRESS sequence. These examples include a general purpose single stopband (highpass) filter for water suppression and lactate methyl proton rephasing, as well as water and lipid bandstop filters targeted for the brain and prostate. The robustness of BASING suppression to B_1 scaling errors was also investigated.

THEORY

BASING is applied after initial RF excitation and consists of a frequency selective 180° RF pulse surrounded by two crusher gradient pulses of opposite signs. Figure 1a shows a single BASING pulse implemented with PRESS excitation. Due to the opposite polarity of the crusher gradients, the spins that are flipped by the BASING pulse are dephased and the spin echo is destroyed. The spins that are not flipped are refocused (albeit with a frequency dependent phase variation) as they experience no net gradient field. If the passband phase variation is simulated, it can be corrected via postprocessing of the spectra.

Alternatively, the passband phase can be made linear by incorporating two identical BASING pulses into the excitation sequence as shown in Fig. 1b. The dual BASING pulses, which are placed on opposite sides of one of the PRESS spin-echo pulses, are phase compensating, which results in an echo forming at the normal PRESS echo time of $TE = 2 \cdot T_{23}$. Dual BASING is similar, in concept, to MEGA (19, 20) which was developed by Mescher and Garwood and initially applied at 4.7 T, using Gaussian shaped inversion pulses, with STEAM (21) excitation.

In this paper, we present and analyze both the single and dual BASING approaches and incorporate SLR pulse design methods to meet specific passband, stopband and transition band design criteria. At 1.5 T, sharp transition bands are required so to optimize passband metabolite (choline, creatine, citrate, NAA, lactate) SNR and achieve adequate suppression while still allowing for sufficient tolerance to B_0 inhomogeneities (22).

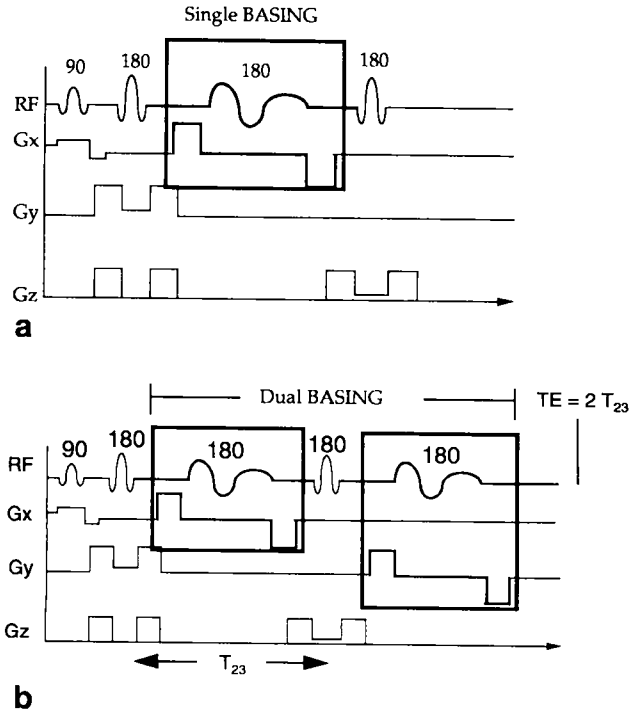

FIG. 1. Single (a) and dual (b) BASING pulses incorporated into the PRESS excitation sequence. The dual BASING scheme is phase compensating with the PRESS echo forming at the normal PRESS echo time of $TE = 2 \cdot T_{23}$ (for $T_{23} > T_{12}$). For the dual BASING scheme, the crusher gradient directions are different for the two pulses.

The SLR algorithm is a powerful tool that allows for the use of linear finite impulse response (FIR) filter design techniques to address the nonlinear RF pulse design problem. RF pulses may be created using the Parks-McClellan (PM) algorithm (23) to produce equiripple filters with excitation profiles possessing specified characteristics including passband and stopband ripple magnitudes (δ_1,δ_2) and transition bandwidths. Pulses with linear, minimum, or maximum phase may be created. Generally, minimum and maximum phase pulses have sharper excitation profiles but, in some cases, are undesirable as they cannot always be completely refocused. Pauly *et al.* (18) derived parameter relations that analytically specify the inputs into the PM algorithm to create (among others) crushed spin-echo (SE) RF pulses. We show that the SE SLR parameter relations also may be used to design BASING pulses and that dual maximum or minimum phase BASING pulses may be completely refocused.

The BASING pulse behavior can be analyzed using the Cayley-Klein parameters (α,β) and the spin domain rotation matrix R:

$$R = \begin{bmatrix} \alpha & -\beta^* \\ \beta & \alpha^* \end{bmatrix} \quad [1]$$

where

$$\alpha = \cos\phi/2 - in_z\sin\phi/2 \quad [2a]$$

$$\beta = -i(n_x + in_y)\sin\phi/2 \quad [2b]$$

The vector $\boldsymbol{n}$ is the axis of rotation and ϕ is the rotation angle of the magnetization vector. The Cayley-Klein parameters are subject to the constraint:

$$\alpha\alpha^* + \beta\beta^* = 1 \quad [3]$$

Starting with the magnetization vector situated in the transverse plane $M_{xy}^- = M_x^- + iM_y^-$, the transverse magnetization M_{xy}^+ resulting from an RF induced rotation (while ignoring T_2 and J-coupling effects) is (from ref. [24]):

$$M_{xy}^+ = (\alpha^*)^2 M_{xy}^- - \beta^2 M_{xy}^{-*} \quad [4]$$

The Cayley-Klein parameters describing a composite rotation comprised of several individual rotations can be calculated by multiplying together consecutive matrices R each describing an individual rotation. For example, by considering an RF induced rotation along with rotations about the z-axis produced by crusher gradients (see below), Pauly *et al.* (18) showed that the profile M_{xy}^+ (SE) of the crushed spin-echo pulse (*positive gradient - RF - positive gradient*) is:

$$M_{xy}^+(\mathrm{SE}) = -\beta^2 M_{xy}^{-*} \quad [5]$$

The excitation profile M_{xy}^+ (BAS) of the BASING pulse (*positive gradient - RF - negative gradient*) can be determined in a similar fashion. The spin-domain rotation matrix R_c representing a rotation induced by a positive B_0

crusher gradient of magnitude G directed along a spatial axis x is

$$R_c = \begin{bmatrix} e^{-i\varphi(x)/2} & 0 \\ 0 & e^{i\varphi(x)/2} \end{bmatrix}, \quad \text{where} \quad \varphi(x) = -x\{\gamma \int G(t)dt\}$$

The rotation matrix associated with a negative crusher of value $-G$ is R_c^*. Using these results for R_c and R_c^* along with R (Eq. [1]), which describes an RF induced rotation, the total BASING rotation matrix R_{BAS} is

$$R_{BAS} = R_c R R_c^* = \begin{bmatrix} \alpha & -\beta e^{-i\varphi(x)} \\ \beta e^{i\varphi(x)} & \alpha^* \end{bmatrix}$$

Using Eq. [4] to relate the resulting transverse magnetization to the matrix elements of R_{BAS}, the profile $M_{xy}^+(BAS)$, after integration across a voxel, is

$$M_{xy}^+(BAS) = (\alpha^*)^2 M_{xy}^- \qquad [6]$$

The absolute value of the BASING magnetization is $|M_{xy}^+(BAS)| = (\alpha\alpha^*)|M_{xy}^-|$ while the SE magnetization magnitude (from Eq. [5]) is $|M_{xy}^+(SE)| = (\beta\beta^*)|M_{xy}^-|$. Hence, from Eq. [3],

$$|M_{xy}^+(BAS)| = 1 - |M_{xy}^+(SE)| \qquad [7]$$

Equation [7] shows that the BASING and SE pulses are complementary and that a *highpass* BASING pulse (one stopband) can be designed using the SLR algorithm to generate a *lowpass* spin-echo (SE) pulse with the SE passband targeted on the region that is to be suppressed (e.g., water). Similarly, a BASING *bandstop* pulse for both water and lipid suppression can be created from an SE *bandpass* filter. The SLR parameter relations must be set properly as the BASING passband and stopband ripple scaling factors, required for input to the PM algorithm, will be switched with those of the SE pulse (see Experimental Methods).

Equation [7] also indicates that the SE and BASING sensitivities to B_1 inhomogeneities are complementary. The SE passband (where the nominal flip angle is 180°) will be more sensitive to RF scaling errors than the BASING passband (where the nominal flip angle is zero). This is consistent with our previously stated design goal of adding pulses to PRESS, which minimally impact the passband metabolites. Conversely, the BASING stopband will be more sensitive than the SE stopband. The effects of B_1 inhomogeneities on the BASING stopband are further discussed later.

The profile M_{xy}^+ (D__BAS) of the dual BASING scheme (Fig. 1b), which consists of a BASING pulse followed by an SE pulse followed by another BASING pulse can be calculated using Eqs. [5] and [6]. For two BASING pulses described by the parameters α_1 and α_2 surrounding an SE pulse described by the parameter β, the resulting dual BASING excitation profile is

$$M_{xy}^+(D\_\_BAS) = -(\alpha_2^*)^2 \beta^2 [(\alpha_1^*)^2 M_{xy}^-]^* \qquad [8]$$

$$= A^2 M_{xy}^+(SE)$$

where $A = \alpha_1 \cdot \alpha_2^*$ is real when $\alpha_1 = \alpha_2$. $M_{xy}^+(SE)$ is given by Eq. [5].

Equation [8] shows that the two BASING pulses are phase compensating when they each have the same excitation profile as governed by α and that the suppression factor is the square of the single pulse BASING suppression factor. Hence, to achieve linear phase, the two BASING pulses need only be identical but not themselves linear phase. This is an important result as it indicates that either maximum or minimum phase BASING pulses may be preferred so to minimize the RF pulse time given ripple amplitude and transition bandwidth specifications. Note that Eq. [8] also shows that as long as one BASING pulse occurs before, and one BASING pulse occurs after the SE pulse, passband phase linearity is achieved. Hence, there is much flexibility in pulse placement.

Using the design guidelines for SLR SE pulses given in Ref. (18) while switching the passband and stopband magnitudes, both single and multi-stopband BASING equiripple FIR filters may be designed with the PM algorithm. Figure 2 shows sample maximum phase BASING RF pulses designed for ^{1}H metabolic imaging at 1.5 T. Also shown are the resulting theoretical magnetization profiles.

The highpass filter, shown in Figs. 2a–2c, suppresses water and, when incorporated into dual BASING, may be used to rephase the lactate methyl doublet (1.3 ppm) independently of *TE* since the *J*-coupled lactate methine quartet (4.1 ppm) is also placed within the inversion band. Using the product operator formalism (25), it is possible to show that the lactate rephasing criteria depend only on the relative placement of the two identical BASING pulses and that *TE*-independent rephasing occurs when the two pulses are separated in time by *TE*/2.

The bandstop filter shown in Figs. 2d–2f suppresses both water and lipids for spectroscopic imaging of the prostate gland. The resonances that are passed include choline (3.2 ppm), creatine (3.0 ppm), and citrate (two overlapping doublets: 2.8–2.5 ppm). The next section describes the pulse designs in more detail.

EXPERIMENTAL METHODS

Several experiments were performed to evaluate BASING and compare it with CHESS and STIR in the brain and prostate. Data were collected using a General Electric (GE) 1.5 T Echo-Speed system (General Electric Medical Systems, Milwaukee WI) equipped with self-shielded gradients (maximum magnitude = 2.2 G/cm). PRESS excitation was used to restrict the selected volume and isotropic 3D phase encoding was used to sample a cube in *k*-space for CSI imaging. The time bandwidth product (TB) of the PRESS slice selective pulses was 7.2. The crusher gradient pulses had a magnitude 2.2 G/cm and were 4.5 ms in duration including the 250 μs rise and decay times. Reconstruction was performed on a SUN SPARC10 using routines for the reconstruction and automatic phasing of spectra (26).

The CHESS water suppression and STIR lipid suppression sequences that were used were part of the GE product software (EPIC 5.5). The CHESS sequence consisted

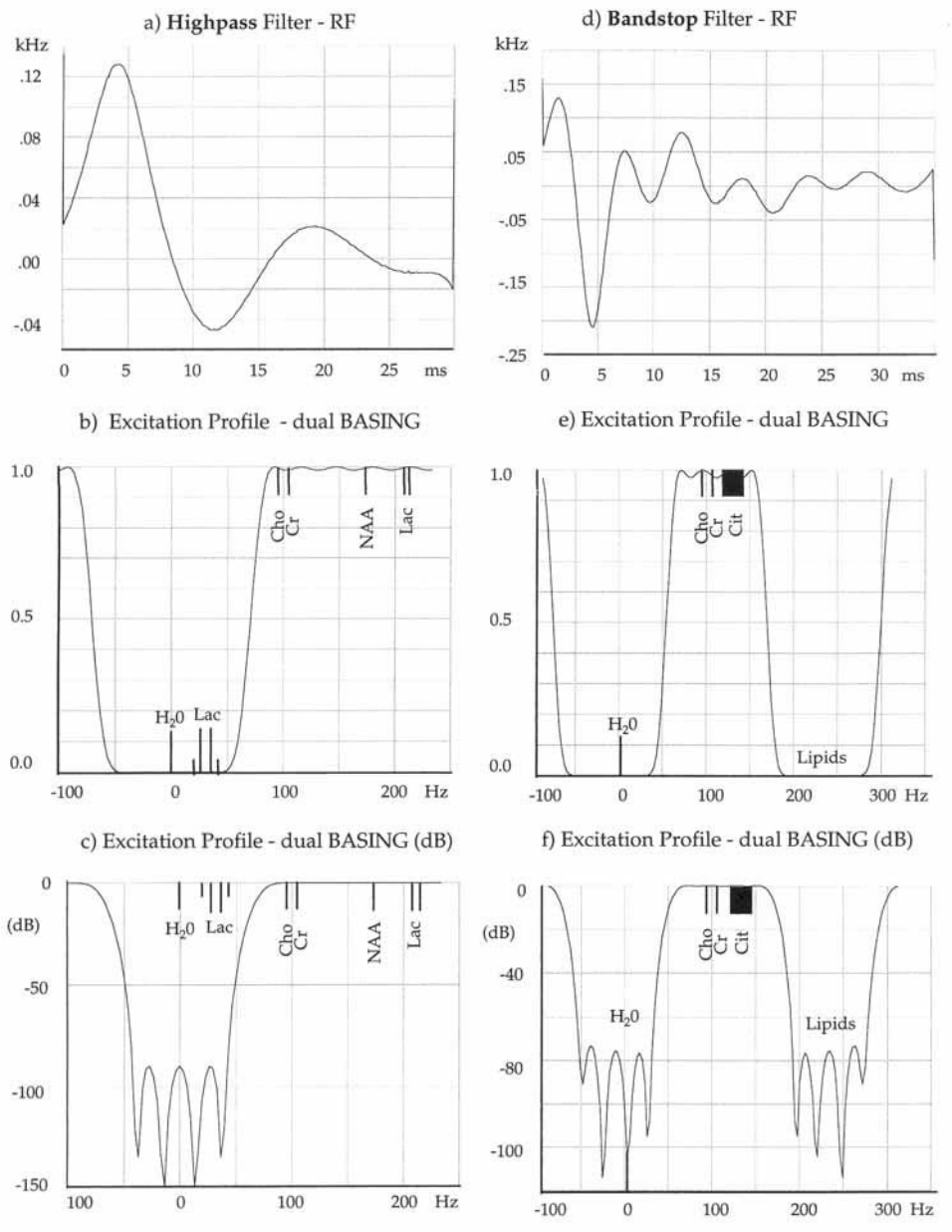

FIG. 2. (a) A maximum phase BASING highpass (one stopband) filter designed to suppress water and rephase the lactate methyl protons, and (b, c) the resulting excitation profile. (d, e, f) A BASING bandstop filter designed to suppress water and lipids in the prostate. The theoretical dual BASING excitation profiles were determined from Eq. [8] under the asumption that M_{xy}^{+} (SE) = 1.

of three consecutive minimum phase pulses each followed by crusher gradients (2.2 G/cm) placed on two axes and that were 14.5 ms in duration. The time bandwidth product (TB) of the pulses was TB = 3.9. For our implementations, we chose a bandwidth bw = 75 Hz. The flip angle of the first and second CHESS RF pulses was set to 90° while the flip angle of the third pulse was adjusted manually to a value between 100° and 130° so to obtain maximum suppression. The *sech/tanh* adiabatic inversion pulse (27) used for STIR (TB = 7.36, bw = 90 Hz, TI = 220 ms) was centered at 1.3 ppm when implemented. Due to potential problems from RF pulse overlap, when STIR was implemented only two CHESS pulses could be applied.

The BASING pulses were designed using an SLR RF pulse package that was written and kindly provided by Dr. John Pauly, Stanford University, and that runs on the MATLAB (MathWorks Inc., Natick, MA) platform. Minor modifications were made to the package that included the addition of multiband filter capabilities as well as specification of the BASING parameter relations. Since, as shown previously, the BASING and SE pulses are complementary (Eq. [7]), the BASING passband and stopband inputs to the Parks-McClellan (PM) algorithm (δ_1^{pm},δ_1^{pm}) were (adapted from Table 1 in ref. 18):

$$\delta_1^{pm} = \sqrt{\delta_1}, \quad \delta_2^{pm} = \delta_2/4$$

where δ_1 and δ_2 are the desired passband and stopband ripple magnitudes. As implemented, the BASING B_0 crusher gradients of opposite signs were of magnitude 2.2 G/cm and duration 4.5 ms.

The design examples include: A) a general purpose highpass filter for water suppression and lactate methyl proton rephasing; B) a water/lipid bandstop filter targeted for the brain designed to pass resonances from choline to NAA; C) a water/lipid bandstop filter targeted for the prostate gland designed to pass choline to citrate resonances. Before human studies were initiated, the BASING excitation profiles were verified with both brain and prostate metabolite 3D CSI phantom experiments.

Dual BASING Highpass Filter for Water Suppression and Lactate Rephasing

The absolute and relative intensities of choline (3.2 ppm), creatine (3.0 ppm), NAA (2.0 ppm), and lactate (1.3 ppm) have been shown to be useful for differentiating between regions of active tumor, normal tissue, and radiation induced necrosis in primary and metastatic brain tumors (28–31). To suppress water and pass the aforementioned metabolites while rephasing the lactate methyl protons, the BASING filter shown in Fig. 2 was developed. The pulse, implemented as part of the PRESS sequence (Fig. 1b), was tested on a brain metabolite

phantom (GE Medical Systems, Milwaukee, WI) and a brain tumor patient.

The water suppression filter, which is shown in Figs. 2a–2c, was 30 ms in duration with a stopband width of 130 Hz (TB = 3.9). To achieve adequate suppression, while minimally impacting on the passband metabolites, the design passband and stopband ripples (δ_1,δ_2) were both set to be 0.5%. After two applications, as required for the dual BASING scheme (Eq. [8]), the final stopband ripple was then δ_2^2 = 0.0025% and passband ripple was approximately $2\delta_1$ = 1% (Figs. 2b, 2c). This allowed for a targeted suppression factor of over 10^4 (80 dB). Using the Parks-McClellan (PM) algorithm for equiripple filter design, the resulting transition bandwidth of the 30 ms maximum phase pulse was 45 Hz. This allowed for +10 Hz tolerance to any B_0 induced frequency shift before the passband choline resonance (3.2 ppm) was attenuated by 5%. Conversely, a −10 Hz frequency shift was allowed before the lactate methine proton (4.1 ppm) inversion factor was reduced by 5%. When implemented on the G.E. Echo-Speed system, the minimum *TE* for PRESS excitation with the BASING pulses was approximately 110 ms.

An experimental profile was generated by applying a small B_0 gradient of value 0.02 G/cm along the *x*-axis during the application of the BASING pulses and imaging the water signal to create an axial projection image of the PRESS selected region. The PRESS box size (*x,y,z*) was 140 × 40 × 20 mm^3. The imaging parameters were *TR* = 1 s, *TE* = 144 ms, acquisition matrix (*x,y*) = 256 × 128, FOV = 18 cm, NEX = 2. With the B_0 test gradient applied, the resolution of the BASING profile was 6.1 Hz/pixel. A profile was calculated by dividing the image acquired with the test gradient applied into one acquired without the gradient applied. In this manner, the effects of B_1 inhomogeneities were removed.

For both phantom and *in vivo* spectroscopy experiments, two sets of CSI spectra were acquired to compare CHESS and BASING water suppression factors. The CSI parameters were *TR* = 1 s, *TE* = 144 ms, NEX = 2, phase encoding steps = 8 × 8 × 8, FOV = 80 mm, resolution = 1 cc, scan time = 17 min. For the phantom data, the PRESS box size was 40 × 40 × 30 mm^3.

The *in vivo* data were acquired from a 34-year-old male brain tumor patient diagnosed with a glioblastoma multiforme. To aid in selecting the location and size of the PRESS excited region, a set of T_1-weighted postcontrast (16 cc Gd-DTPA) 3D SPGR images (*TR* = 26 ms, *TE* = 6 ms, flip angle = 40°, 1.5-mm resolution) was first acquired and reconstructed. The location of the PRESS selected region (40 × 60 × 40 mm^3) was chosen based upon the imaging results. As the Gd-DTPA increases the amount of local T_1 variation of water, it also renders CHESS suppression less effective.

Single BASING Bandstop Filter for Water and Lipid Suppression in the Brain

In cases where the region of interest is in close proximity to the skull, it may be desired to suppress both water and lipids in the brain. Figure 3 shows a minimum phase BASING bandstop pulse designed to pass choline to

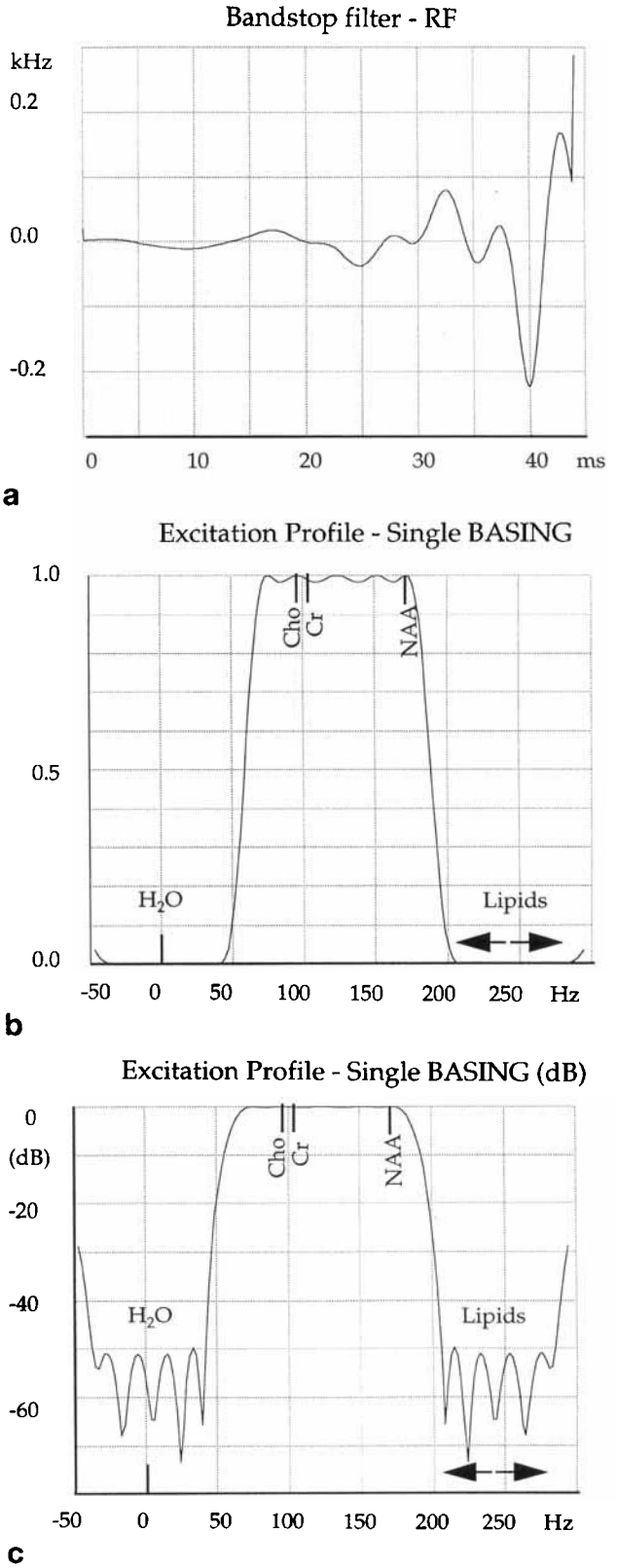

FIG. 3. A 44-ms minimum phase BASING pulse designed for water and lipid suppression in the brain at 1.5 T (a) and the corresponding excitation profile (b, c). The transition bandwidth is 30 Hz allowing for the suppression of most lipids while passing NAA.

NAA resonances and suppress lipids. The pulse length was 44 ms with 3% passband and 0.25% stopband ripple. The passband width was 150 Hz and the stopband widths were 125 Hz. The transition bandwidth was 30 Hz which is sufficient to pass NAA and attenuate most lipid protons. A +5 Hz shimming tolerance was allowed before a 5% reduction of the NAA signal occurred and a −25 Hz tolerance was allowed before a 5% reduction of the choline signal. Using this pulse on the G.E. Echo-Speed system, the minimum *TE* was approximately 120 ms.

A normal volunteer was scanned first with the 3D SPGR imaging sequence (*TR* = 26 ms, *TE* = 6 ms, flip angle = 40°, 1.5-mm resolution) followed by two PRESS CSI acquisitions. The PRESS excitation box (45 × 45 × 40 mm^3) was placed near the left lateral and superior part of the head. As it was desired to include as much brain parenchyma as possible, some slices in the superior part of the PRESS box were contaminated with subcutaneous lipid signals due to the curvature of the skull.

Two sets of 3D CSI spectra were acquired. For the first CSI data set, the three-pulse CHESS manually optimized sequence was used for water suppression. The second data set was acquired with the three-pulse nonoptimized CHESS sequence along with the single BASING bandstop pulse (Fig. 3). For both CSI acquisitions, the scanning parameters were *TR* = 1 s, *TE* = 144 ms, NEX = 2, phase encoding = 8 × 8 × 8, FOV = 80 mm, resolution = 1 cc, scan time = 17 min.

Dual BASING Bandstop Filter for Water and Lipid Suppression in the Prostate Gland

^1H CSI in the prostate offers several promising applications as information drawn from choline+creatine to citrate ratios may provide a reliable means of identifying regions of active tumor (32). Spectroscopic imaging of the prostate requires both water and lipid suppression since periprostatic fat surrounds much of the gland. Frequency selective lipid suppression is more propitious at 1.5 T in the prostate than in the brain as the citrate chemical shift (two overlapping doublets ranging from 2.5–2.8 ppm) is 60–90 Hz downfield of most of the lipid resonances.

For prostate MRSI, a 35-ms bandstop BASING pulse was designed with a passband width of 125 Hz and stopband widths of 120 Hz and is shown in Fig. 2. The design passband ripple magnitude was 2% and stopband ripple magnitudes were 0.006% after two applications as required for the dual BASING scheme. The pulse had a transition bandwidth of ~35 Hz, which allowed for a +25/−15 Hz shimming tolerance before a 5% attenuation of the passband metabolites occurred.

3D PRESS CSI using the expandable MRInnervu endorectal surface coil (Medrad Inc., Pittsburgh, PA) in combination with a pelvic phased array coil (G.E. Medical Systems, Milwaukee, WI) operating in receive only mode was performed to compare CHESS and STIR with dual BASING in a phantom and *in vivo*. The metabolite phantom was comprised of choline (4 m*M*), creatine (12 m*M*), and citrate (15 m*M*) dissolved in 9% NaCl and buffered to pH 6.5. The *in vivo* scans were performed on a 55-year-old male. The MRS imaging parameters were *TR* = 1 s, *TE* = 130 ms, NEX = 2, phase encoding steps = 8 × 8 × 8, FOV = 50 mm, resolution = 0.24 cc, scan time = 17 min. For the phantom data, the PRESS box size was 37.0 × 22.0 × 18.0 mm^3. For the *in vivo* scan, the PRESS box dimensions were 44.5 × 19.5 × 18.0 mm^3. Due to constraints associated with implementation of the STIR pulse, the CHESS sequence consisted of only two minimum phase SAT pulses with the flip angle of the second pulse manually adjusted.

EXPERIMENTAL RESULTS

Dual BASING Highpass Filter for Water Suppression and Lactate Rephasing

Figure 4 shows results from the brain phantom experiments. Figure 4a shows the axial water image acquired using the dual BASING sequence with the test B_0 gradient applied along the *x* axis. Figure 4b shows the measured profile calculated by averaging the center 30 rows of the image in Fig. 4a and dividing the result into an average of the center 30 rows of an image acquired without the test gradient. The experimental profile matches the theoretical profile shown in Fig. 2b.

Figures 4c and 4d show representative spectra from the CHESS and the dual BASING phantom CSI experiments. Using the dual BASING scheme, the measured water suppression factor was over 10^4 and no residual water signal was evident. The lactate methyl protons were rephased and upright as shown Fig. 4d. As the BASING spectra were successfully phased with a zero order correction, this indicates that the dual BASING scheme yielded a linear passband phase with an echo time $TE = 2 \cdot T_{23}$ when incorporated into PRESS. At a *TE* of 144 ms (1/*J*), the lactate peaks acquired without BASING were inverted due to *J*-coupling effects (Fig. 4c). The average choline, creatine and NAA metabolite peak height signal to noise ratios taken from 48 voxels in both data sets were virtually identical (dual BASING: 28.7, CHESS: 27.3).

Figure 5 shows the *in vivo* results from the brain tumor scan. Here, there were larger B_1 and T_1 variations and the residual CHESS water peak heights (Fig. 5b) were, in places, over 30 times those of the metabolite peak heights. In comparison, the BASING suppressed water was reduced by up to an additional factor of 200 to levels indistinguishable from the noise (Fig. 5d). Even though the stopband width of the CHESS suppression pulses (75 Hz) was less than that of the BASING pulses (130 Hz), the B_0 field homogeneity was sufficient to analyze 93 voxels for comparison. For these 93 voxels, the residual water peaks were frequency shifted by less than ± 8 Hz, i.e., well within both the CHESS and BASING stopbands.

For the 93 voxels analyzed, the mean residual CHESS magnitude water peak height was 17 times the mean metabolite (choline, creatine, NAA) peak heights. There was significant variability in the amount of suppression achieved as the maximum water to mean metabolite peak height ratio was 57 and minimum was 1.3. In comparison, for a majority of the BASING voxels, the residual water was indistinguishable from the noise. Only 10 out of the 93 BASING voxels possessed a noticeable water signal, which was of the order of the metabolites. A

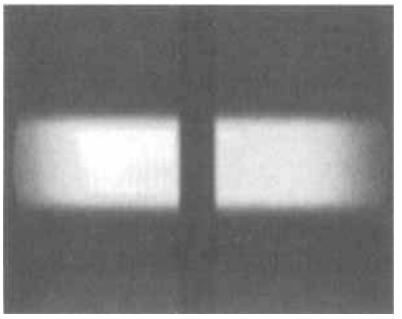

a

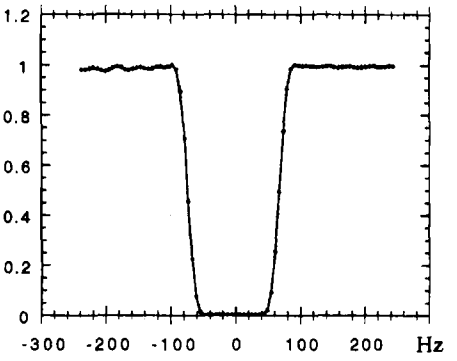

b

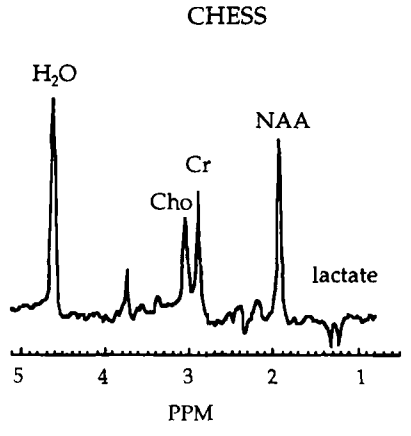

c

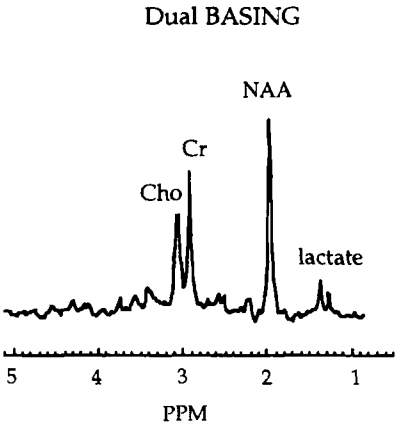

d

FIG. 4. (a) Axial projection of the PRESS box (*TR/TE* = 2000/144) acquired to assess the frequency response of the highpass BASING pulse. A B_0 test gradient directed along the *x* axis was applied simultaneously with the BASING pulses, (b) Measured profile constructed by dividing the image in (a) into an image acquired without the test gradient applied. 1 cc CSI voxels (*TR/TE* = 1000/144) from a ^{1}H brain metabolite phantom scanned with a three-pulse manually optimized CHESS water suppression sequence (c) and with the dual BASING highpass filter (d). Using dual BASING, the water was completely removed and the methyl lactate resonances were rephased and upright.

nonlocalized FID was also acquired using the same excitation parameters and the overall residual BASING water peak height was less than one half the overall metabolite peak heights.

The impact of the improved suppression can be seen in the highlighted zoomed absorption spectra (Figs. 5c, 5e), which were automatically phased. While the BASING-suppressed spectrum exhibited no baseline offset associated with residual water, the CHESS spectrum was considerably distorted as the choline base was situated near the peak of the NAA signal.

Single BASING Bandstop Filter for Water and Lipid Suppression in the Brain

Figure 6 shows results from the experiment using a single BASING pulse with a sharp transition band to augment both water and lipid suppression in the brain. With the inclusion of BASING, the resconstructed magnitude spectra were free of lipids and water even for voxels in close proximity to the skull where the decrease in residual lipid peak heights was over two orders of magnitude. Although Fig. 4 only shows data from one slice of the 3D data set, baseline artifacts were removed from all four slices that comprised the PRESS excited region.

Dual BASING Bandstop Filter for Water and Lipid Suppression in the Prostate Gland

For the prostate metabolite phantom acquisitions, the measured mean (choline, creatine, citrate) SNR was virtually identical for CHESS and STIR compared with dual BASING. (CHESS + STIR SNR = 17.0, Dual BASING SNR = 16.8).

Figure 7 shows the *in vivo* imaging and spectroscopy results. The T_2-weighted image was corrected using a routine that compensates for the theoretical profile of the surface coil (33). The spectra show that, with dual BASING, both the residual water and lipid signals were reduced to background noise levels and there were no baseline artifacts. In comparison, with STIR and manually optimized CHESS, the residual water and lipid peak heights were up to 25 times and 6 times the metabolite peak intensities, respectively. This caused significant baseline distortion for the automatically phased spectra. Note that, even though the maximum residual lipid peak intensity using STIR was only 6 times the metabolite intensities, this still caused baseline errors due to the relatively large line-widths of the lipids and their close proximity to citrate. While the BASING data displayed no significant residual water or lipid peaks that were located within the stopbands, there were residual broad resonances present between 2.3 and 2.0 ppm, which is within a BASING transition band. These resonances were most likely comprised of methylene lipids but may also have included glutamine, glutamate, and polyamines.

DISCUSSION

The BASING pulse has been shown to be complementary to the spin-echo (SE) pulse and offers an effective means of achieving T_1-independent solvent suppression with minimal impact on the passband metabolites. BASING also may have unique applications to weakly coupled systems such as lactate. Our results demonstrate that both dual or single BASING implementations may be used for water and/or lipid suppression. The dual BAS-

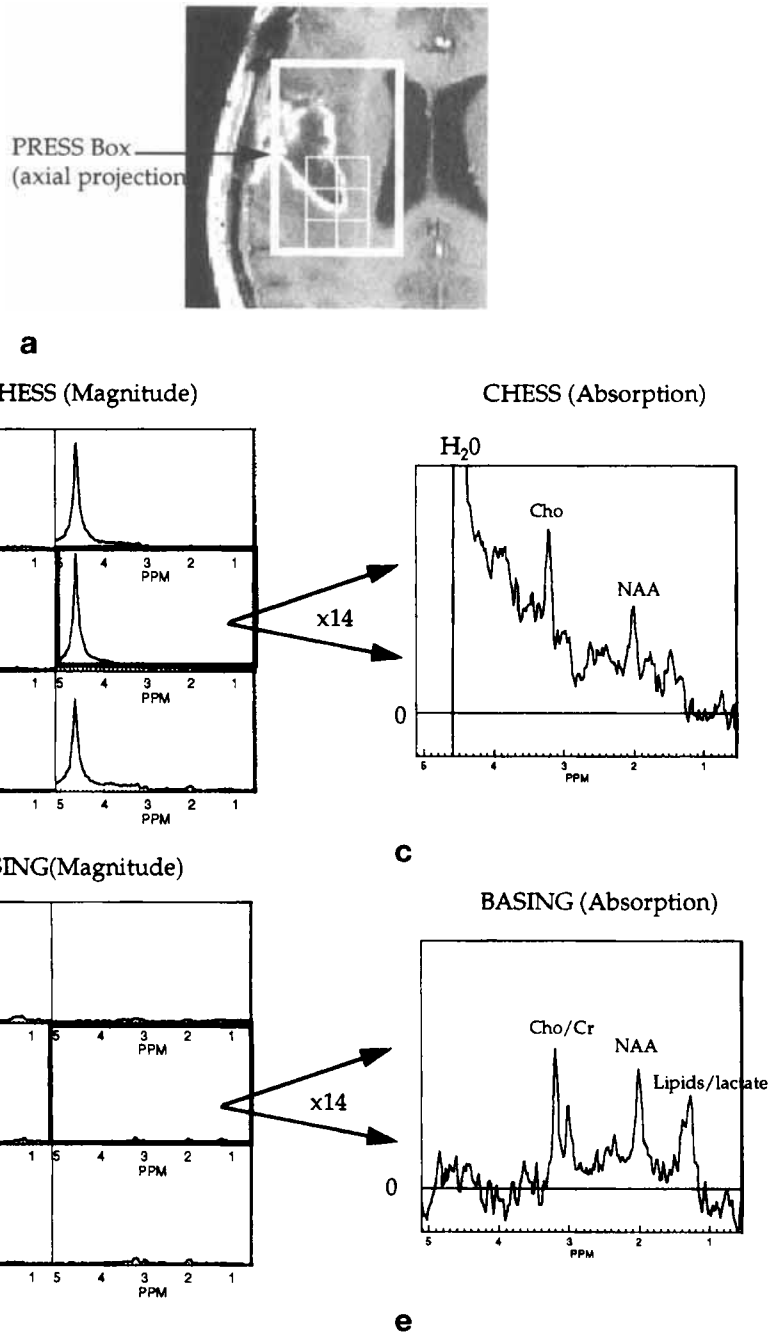

FIG. 5. Comparison of the three pulse manually optimized CHESS water suppression scheme with dual BASING over a selected region in a brain tumor patient. (a) Axial projection of the PRESS selected volume and part of the CSI reconstruction grid superimposed over a corresponding postcontrast T_1-weighted SPGR (*TR/TE* = 26/6) 3 mm thick slice. (b) CHESS magnitude spectra for the six voxels highlighted in (a). (c) Absorption spectrum from the single highlighted voxel zoomed by a factor of 14. (d) Six corresponding BASING magnitude spectra scaled the same as in b. (e) Zoomed BASING absorption spectrum. The replacement of CHESS suppression with BASING resulted in the complete elimination of the water signal and decreased baseline artifacts. For all spectral acquisitions, *TR/TE* = 1000/144.

ING scheme seems generally advantageous due to its improved suppression factors and resulting linear passband phase.

Experimental results demonstrated that BASING may be used to either augment or replace CHESS and STIR suppression sequences. This can result in substantial time savings by eliminating the need to optimize CHESS flip angles and has allowed for the study of regions of interest where residual water and/or lipid resonances would overwhelm the peaks of interest. The phantom data showed that there was no observable SNR decrease associated with using BASING which suggests that such potentially deleterious effects as signal losses resulting from diffusion or RF hardware imperfections were minimal. To date, we have performed over 150 patient studies using BASING suppression and have noticed no adverse effects of the pulse on passband SNR. However, in theory, due to the long duration of the applied pulses, the BASING sequence can be susceptible to motion artifacts.

The BASING highpass filter was shown to be useful for water suppression and lactate rephasing and may be applicable to many parts of the body aside from the brain. *In vivo*, the water suppressed spectra acquired with the BASING highpass filter displayed residual stopband signals which were well below the levels of the metabolites. A suppression factor improvement of over 200 was demonstrated compared with a three pulse manually optimized CHESS sequence. This reduction in water signal intensity reduced baseline artifacts thus enabling more robust quantification of metabolite levels. The data also suggest a potential application of lactate editing. As the dual BASING implementation successfully rephases the lactate methyl protons while minimally impacting on the lipids that are far off the stopband resonance, it may be incorporated into a T_2-independent *J*-difference editing scheme (34, 35) for an echo time of $TE = 1/J$.

In the brain, a bandstop pulse may be used for both water and lipid suppression where the voxel of interest includes subcutaneous fat. Experimental data showed complete removal of baseline artifacts with the single BASING implementation used to augment CHESS (See

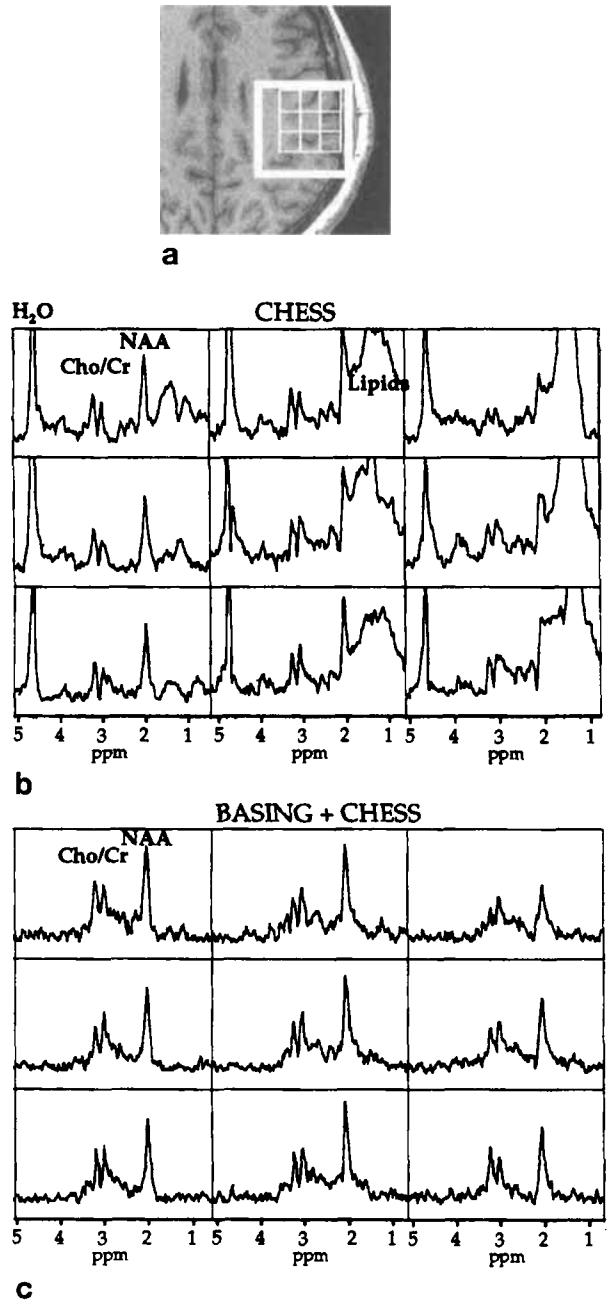

FIG. 6. ^1H data sets acquired from a normal volunteer with the PRESS box situated close to the skull. (a) Axial projection of the PRESS selected volume and part of CSI reconstruction grid superimposed on a SPGR (*TR/TE* = 26/6) 3-mm thick slice. Magnitude spectra (*TR/TE* = 1000/144) acquired with manually optimized CHESS and OVS (b) and Single BASING + nonoptimized CHESS + OVS (c). Incorporation of the BASING pulse effectively removed all baseline artifacts resulting from the water and lipids.

Fig. 6). To pass NAA and attenuate lipid resonances at 1.5 T, the required passband to stopband transition width was found to be 30 Hz. To achieve this narrow transition band, a 44 ms minimum phase BASING pulse was required. Although, the minimum *TE* increased to 120 ms, this still allowed us to scan with our normal protocol of *TE* = 144 ms. However, the shimming tolerances of ±5 Hz were restrictive, which may hinder implementation for large volumes of interest at 1.5 T. At higher fields, these concerns may be reduced since the required duration of the BASING pulse scales inversely with the field strength thus allowing for shorter echo times and/or larger tolerances for B_0 inhomogeneities. In cases where adequate lipid suppression may be obtained using oblique outer volume suppression bands (OVS) (11, 36, 37) or with STIR (38), the BASING highpass filter can be used for water suppression and lactate rephasing.

In the prostate, it is essential to suppress both water and fat as the gland is surrounded by adipose tissue located very close to the region of interest. Frequency selective lipid suppression is more practical for prostate MRS than brain MRS since, at 1.5T, the citrate peaks are situated 30-50 Hz further downfield of the lipids than is NAA. Moreover, due to *J*-modulation effects, the optimal citrate *TE* is approximately 130 ms (32, 39, 40). Thus, the addition of BASING pulses to the PRESS sequence does not negatively impact the minimal practical echo time. The experimental data presented demonstrate that bandstop BASING pulses may be used to completely remove primary water and lipid resonances (see Fig. 7). However, there were still residual unsuppressed signals situated close to the citrate resonances which were within the filter transition band and which can affect the baseline. The origin of these signals must still be investigated and the effect of the BASING pulse on these broad resonances must still be evaluated.

Although the BASING passband is relatively insensitive to B_1 errors, the suppression factor remains B_1-dependent, but less so than for the saturation pulses that are used for CHESS. Figure 8 shows a plot of suppression factor (dB) versus B_1 scaling error for dual BASING and dual SAT pulses as might be used for CHESS or OVS (no T_1 considerations). The suppression calculations were performed using the spin domain formalism while assuming that the design stopband ripple amplitudes are zero. BASING is shown to be significantly more robust. For example, for a 10% scaling error, the dual BASING suppression factor is over 60 dB while the dual SAT is less than 35 dB. T_1 considerations will further reduce the effectiveness of the SAT pulses. A disadvantage of BASING is that longer *TE*s are required.

The dual BASING scheme also may be applied to single echo localization sequences such as required for 2D CSI. Although excellent water suppression has been achieved using frequency selective rephasing as with the BASSALE *cos-sinc* pulse (11) or an optimized pulse (12), it may be desired that both the excitation and spin-echo pulses be slice selective. This is a necessity for interleaved 2D CSI (38) where more than one slice per *TR* is acquired. Previously, this problem has been addressed through the use of spectral/spatial echo-planar spin-echo (EPSE) excitation (41). However, in many cases, EPSE excitation may not always be practical to implement due to B_0 gradient hardware (slew rate and magnitude) and B_1 peak power constraints. Moreover, as the B_0 field strength increases, both the gradient and RF capabilities must increase as well. A practical alternative to EPSE suppression for interleaved 2D CSI, especially at higher f ields, may be to use dual BASING with the

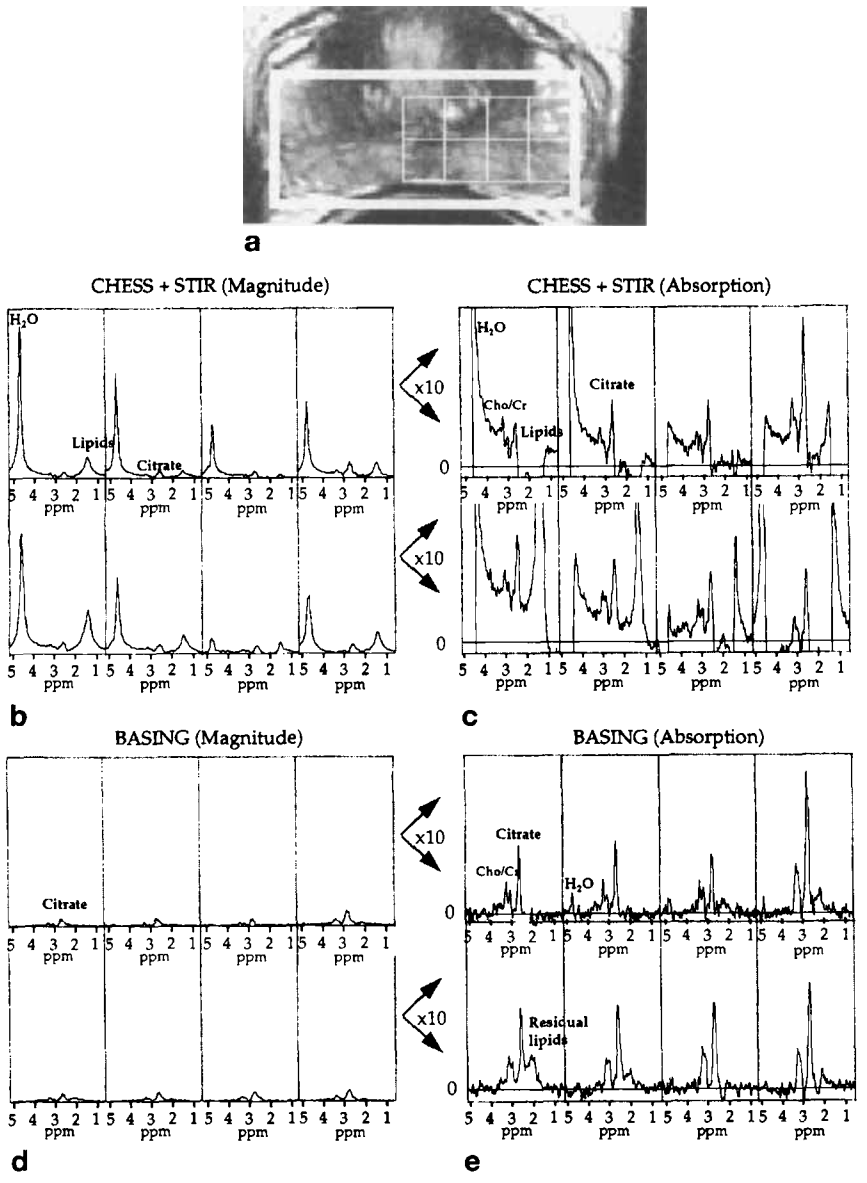

FIG. 7. Comparison of CHESS and STIR suppression with BASING in the prostate (*TR/TE* = 1000/130). (a) The PRESS box and part of CSI reconstruction grid superimposed upon an axial T_2-weighted (*TR/TE* = 5000/102) 3-mm thick slice; (b, d) Magnitude spectra showing water and lipid levels with CHESS and BASING; (c, e) Automatically phased absorption spectra zoomed by a factor of 10. With dual BASING, baseline artifacts were eliminated although there remained some residual resonances (~2.1 ppm), which may have arisen from methylene lipids located within the filter transition band.

slice selective excitation and SE pulses applied along the same axis.

SUMMARY

A new solvent suppression scheme (BASING) has been introduced and applied to ^{1}H spectroscopic imaging. Both single- and multi-bandstop filters, generated using the Shinnar Le-Roux transform, were used to suppress water and lipids and in the brain and prostate at 1.5 T. Residual stopband resonances and associated baseline artifacts were eliminated as the suppression factor was improved by over two orders of magnitude over that provided by CHESS and STIR sequences. Although, the implementation of the BASING scheme increased the minimum *TE*, the echo time was still short enough to conform to our current protocols. Shorter echo times are expected to be achieved at higher fields. While the examples presented in this paper incorporated BASING

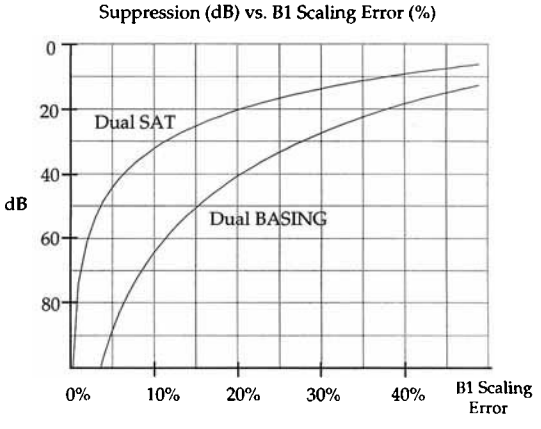

FIG. 8. Dual SAT and dual BASING suppression factors plotted as a function of B_1 scaling error. T_1 effects were not taken into account for the dual SAT calculations. Dual BASING suppression is shown to be significantly more robust.

into PRESS localization, BASING also may be used with other sequences such as interleaved 2D CSI.

ACKNOWLEDGMENTS

The authors thank Dr. John Pauly for making available his MATLAB SLR RF pulse design package through NIH Research Resources Grant 1 P41 RR09784. The authors also thank Lucas Carvajal, Mark Day, Dr. Roland Henry, Sue Noworolski and Dr. Lawrence L. Wald for helpful discussions and use of their image display and processing routines, as well as the members of the GE Signa Spectroscopy Group at Fremont for their support in sequence development.

REFERENCES

1. T. R. Brown, B. M. Kincaid, K. Ugurbil, NMR chemical shift imaging in three dimensions. *Proc. Natl. Acad. Sci. USA* **79,** 3523–3526 (1982).
2. A. A. Maudsley, S. K. Hilal, H. E. Simon, S. Wittekoek, *In vivo* MR spectroscopic imaging with P-31. Work in progress. *Radiology* **153,** 745–750 (1984).
3. S. J. Nelson, M. R. Day, L. Carvajal, S. E. Moyher, D. Meaney, R. Henry, L. L. Wald, D. B. Vigneron, Methods for analysis of serial volume MRI and ^{1}H MRS data for the assessment of response to therapy in patients with brain tumors, *in* "Proc., SMR, 3rd Annual Meeting, Nice, France, 1995," p. 1960.
4. J. Kurhanewicz, H. Hricak, D. Vigneron, S. Nelson, F. Parivar, K. Shinohara, P. Carroll, Following metabolic response to prostate cancer cryosurgery by 3D MRSI. *Radiology* **200(2),** 489–496 (1996).
5. J. Kurhanewicz, D. Vigneron, H. Hricak, P. Carroll, P. Narayan, S. Nelson, Three-dimensional H-1 MR spectroscopic imaging of the in situ human prostate with high (0.24–0.7-cm^3) spatial resolution. *Radiology* **198,** 795–805 (1996).
6. P. A. Bottomley, Spatial localization in NMR spectroscopy *in vivo*. *Ann. N.Y. Acad. Sci.* **508,** 333–348 (1987).
7. A. Haase, J. Frahm, W. Hanicke, D. Matthaei, ^{1}H NMR chemical shift selective (CHESS) *imaging. Phys. Med. Biol.* **30,** 341–344 (1985).
8. G. Bydder, I. Young, MR imaging: clinical use of the inversion recovery sequence. *J. Comput. Assist. Tomogr.* **9,** 659–675 (1985).
9. R. Ogg, P. Kingsley, J. W. E. T. Taylor, a T1- and B1- insensitive water-suppression method for in vivo localized ^{1}H NMR spectroscopy. *J. Magn. Reson. B* **104,** 1–10 (1994).
10. T. Ernst, J. Hennig, Improved water suppression for localized in vivo 1H spectroscopy. *J. Magn. Reson. B* **106,** 181–6 (1995).
11. D. C. Shungu, J. D. Glickson, Band-selective spin echoes for in vivo localized 1H NMR spectroscopy. *Magn. Reson. Med.* **32,** 277–84 (1994).
12. H. P. Hetherington, J. W. Pan, G. F. Mason, S. L. Ponder, D. B. Twieg, G. Deutsch, J. Mountz, G. M. Pohost, 2D ^{1}H spectroscopic imaging of the human brain at 4.1 T. *Magn. Reson. Med.* **32,** 530–534 (1994).
13. V. Sklenar, M. Piotto, R. Leppik, V. Saudek, Gradient-tailored water suppression for ^{1}H-15N HSQC experiments optimized to retain full sensitivity. *J. Magn. Reson. A* **102,** 241–5 (1993).
14. C. Dalvit, S. Y. Ko, J. M. Bohlen, Single and multiple-selective excitation combined with pulsed field gradients. *J. Magn. Reson. B* **110,** 124–31 (1996).
15. H. Tsang-Lin, A. J. Shaka, Water suppression that works. Excitation sculpting using arbitrary waveforms and pulsed field gradients. *J. Magn. Reson. A* **112,** 275–279 (1995).
16. M. Shinnar, L. Bolinger, J. S. Leigh, The use of finite impulse response filters in pulse design. *Magn. Reson. Med.* **12,** 81–87 (1989).
17. P. Le Roux, Exact synthesis of radio frequency waveforms, *in* "Proc., SMRM, 7th Annual Meeting, San Francisco, 1988," p. 1049.
18. J. Pauly, P. Le. Roux, D. Nishimura, A. Macovski, Parameter relations for the Shinnar Le-Roux RF Design Algorithm. *IEEE Trans. Med. Imaging* **10,** 53–65 (1991).
19. M. Mescher, M. Garwood, Solvent suppression using selective echo dephasing, *in* "Proc., 37th Experimental Nuclear Magnetic Resonance Conference, Pacific Grove, California, 1996," p. 236.
20. M. Mescher, A. Tannus, M. O'Neil Johnson, M. Garwood, Solvent suppression using selective echo dephasing. *J. Magn. Reson. A* **123,** 226–229 (1996).
21. J. Frahm, H. Bruhn, M. L. Gyngell, K. D. Merboldt, W. Hanicke, R. Sauter, Localized high-resolution proton NMR spectroscopy using echoes: initial applications to human brain *in vivo*. *Magn. Reson. Med.* **9,** 79–93 (1989).
22. P. G. Webb, N. Sailasuta, S. J. Kohler, T. Raidy, R. A. Moats, R. E. Hurd, Automated single-voxel proton MRS: technical development and multisite verification. *Magn. Reson. Med.* **169,** 207–212 (1994).
23. A. V. S. R. W. Oppenheim, Discrete Time Signal Processing (Prentice Hall, Englewood Cliffs, N.J., (1989)).
24. E. T. Jaynes, *Matrix treatment of nuclear induction. Phys. Rev.* **74,** 226–263 (1955).
25. O. W. Sorensen, G. W. Eich, R. R. Ernst, Product Operator Formalism for the Description of NMR Pulse Experiments. *Prog. NMR Spectrosc.* **16,** 163–192 (1983).
26. S. J. Nelson, T. R. Brown, A New Method for Automatic Quantification of 1D Spectra with Low Signal to Noise Ratio. J. Magn. Reson. **75,** 229–243 (1987).
27. M. S. Silver, R. I. PA Joseph, D. I. PA Hoult, Selective spin inversion in nuclear magnetic resonance and coherent optics through an exact solution of the Bloch-Riccati equation. *Phys. Rev. A* **31,** 2753–5 (1985).
28. H. Bruhn, J. Frahm, M. L. Gyngell, K. D. Merboldt, W. Hanicke, R. Sauter, C. Hamburger, Noninvasive differentiation of tumors with use of localized H-1 MR spectroscopy in vivo: initial experience in patients with cerebral tumors [see comments]. *Radiology* **172,** 541–8 (1989).
29. J. H. Langkowski, J. Wieland, H. Bomsdorf, D. Leibfritz, M. Westphal, W. Offermann, R. Maas, Pre-operative localized in vivo proton spectroscopy in cerebral tumors at 4.0 Tesla–first results. *Magn. Reson. Imaging* **7,** 547–55 (1989).
30. J. R. Alger, J. A. Frank, A. Bizzi, M. J. Fulham, B. X. DeSouza, M. O. Duhaney, S. W. Inscoe, J. L. Black, Z. P. van, C. T. Moonen, a. l. et, Metabolism of human gliomas: assessment with H-1 MR spectroscopy and F-18 fluorodeoxyglucose PET [see comments]. *Radiology* **177,** 633–41 (1990).
31. L. Chang, D. McBride, B. L. Miller, M. Cornford, R. A. Booth, S. D. Buchthal, T. M. Ernst, D. Jenden, Localized in vivo 1H magnetic resonance spectroscopy and in vitro analyses of heterogeneous brain tumors. *J. Neuroimaging* **5,** 157–63 (1995).
32. J. Kurhanewicz, R. Dahiya, J. M. Macdonald, L. H. Chang, T. L. James, P. Narayan, Citrate alterations in primary and metastatic human prostatic adenocarcinomas: 1H magnetic resonance spectroscopy and biochemical study. *Magn. Reson. Med.* **29,** 149–57 (1993).
33. S. E. Moyher, D. B. Vigneron, S. J. Nelson, Surface coil MR imaging of the human brain with an analytic reception profile correction. *J. Magn. Reson. Imaging* **5,** 139–44 (1995).
34. D. L. Rothman, K. L. Behar, H. P. Hetherington, R. G. Shulman, Homonuclear 1H double-resonance difference spectroscopy of the rat brain in vivo. *Proc. Natl. Acad. Sci. USA.* **81,** 6330–6334 (1984).
35. H. P. Hetherington, M. J. Avison, R. G. Shulman, 1H homonuclear editing of rat brain using semiselective pulses. *Proc. Natl. Acad. Sci. USA* **82,** 3115–3118 (1985).
36. S. Singh, B. K. Rutt, R. M. Henkelman, Projection presaturation: a fast and accurate technique for multidimensional spatial localization. *J. Magn. Reson.* **87,** 567–83 (1990).
37. J. H. Duijn, G. B. Matson, A. A. Maudsley, M. W. Weiner, 3D phase encoding 1H spectroscopic imaging of human brain. *Magn. Reson. Imaging* **10,** 315–9 (1992).
38. D. M. Spielman, J. M. Pauly, A. Macovski, G. H. Glover, D. R. Enzmann, Lipid-suppressed single- and multisection proton spectroscopic imaging of the human brain. *J. Magn. Reson. Imaging* **2,** 253–62 (1992).
39. F. Schick, H. Bongers, S. Kurz, W. I. Jung, M. Pfeffer, O. Lutz, Localized proton MR spectroscopy of citrate in vitro and of the prostate in vivo at 1.5 T. *Magn. Reson. Med.* **29,** 38–43 (1993).
40. R. V. Mulkern, J. L. Bowers, Calculating spectral modulations of AB systems during PRESS acquisitions [letter; comment]. *Magn. Reson. Med.* **30,** 518 (1993).
41. J. Pauly, D. Spielman, A. Macovski, Echo-planar spin-echo and inversion pulses. *Magn. Reson. Med.* **29,** 776–82 (1993).